Università degli Studi di Padova

Dipartimento di Salute della Donna e del Bambino

SCUOLA DI DOTTORATO DI RICERCA IN : MEDICINA DELLO SVILUPPO e SCIENZE DELLA PROGRAMMAZIONE

INDIRIZZO: MALATTIE RARE, GENETICA, BIOLOGIA e BIOCHIMICA

CICLO XXVI

MOUSE AMNIOTIC FLUID STEM CELLS ARE ABLE TO DIFFERENTIATE INTO SATELLITE CELLS REPLENISHING THE DEPAUPERATED MUSCLE STEM CELL NICHE

Direttore della Scuola : Ch.mo Prof. Giuseppe Basso

Coordinatore d'indirizzo: Ch.mo Prof. Giorgio Perilongo

Supervisore: Ch.ma Prof.ssa Chiara Messina

Dottorando: Martina Piccoli

Abbreviations

AFS: amniotic fluid stem cells

BM: bone marrow

Ctx: cardiotoxin

EDL: *extensor digitorum longus*

ES: embryonic stem cells

FL: fetal liver

GFP: green fluorescent protein

PCR: polymerase chain reaction

pt: post transplantation

SC: satellite cells

SMA: spinal muscular atrophy

SMN: survival motor neuron gene

TA: *tibialis anterior*

WT: wild type

Table of content

i. **Riassunto** 3

ii. **Abstract** 7

iii. **Introduction** 11

1. Amniotic fluid stem cells
2. Spinal muscular atrophy mouse model

iv. **Aim** 17

v. **Materials and methods** 19

1. Mice
2. Amniotic fluid collection and stem cell selection
3. Flow cytometry analysis
4. Bone marrow collection
5. Fetal liver cells isolation and selection
6. AFS cell expansion
7. Cell injection
8. Secondary transplants
9. In vivo imaging
10. Muscle physiology, histology, and immunofluorescence analyses
11. Image processing
12. Western blot
13. RNA extraction and Real Time PCR
14. DNA extraction and PCR analyses
15. Statistical analyses

vi. **Results** 25

1. Mouse AFS cell characterization
2. AFS cell transplantation in mild muscular atrophy mouse model
3. Restoration of muscle phenotype after AFS cell transplantation

4. AFS cells engraft in the muscle stem cell niche and express satellite cell markers
5. *In vitro* expanded AFS cells preserve myogenic potential

vii. Discussion **41**

viii. Bibliography **47**

i. Riassunto

Introduzione: Negli ultimi anni lo studio delle cellule staminali ha suscitato molto interesse, sia per il grande potenziale di queste cellule nelle terapie e applicazioni cliniche, sia come modello di studio *in vitro* per diversi tipi di malattie. In particolare, le cellule staminali embrionali hanno una elevata capacità proliferativa e di differenziazione, ma il loro utilizzo è ancora associato a problematiche etiche. Anche le cellule staminali adulte possiedono grandi potenzialità differenziative sia *in vitro* che *in vivo*, tuttavia il loro utilizzo è limitato in quanto difficili da isolare ed espandere, soprattutto in ambito clinico. In questo scenario sarebbe vantaggioso poter ottenere una popolazione di cellule con elevata capacità di proliferazione e differenziazione, senza dover affrontare però problemi di tipo etico. Nel 2007 il nostro gruppo ha isolato una popolazione di cellule staminali dal liquido amniotico (cellule AFS), utilizzando come marcatore il recettore c-Kit. Queste cellule hanno capacità clonogenica e possono essere dirette a differenziare in una vasta gamma di tipi cellulari appartenenti a tutti e tre i foglietti germinativi.

Obiettivo: Questo lavoro mira a caratterizzare il potenziale miogenico delle cellule staminali del liquido amniotico di topo utilizzando un modello murino di atrofia spinale muscolare. In particolare è volto ad analizzare la capacità delle cellule AFS di dare origine a cellule staminali muscolari e colonizzare la nicchia staminale del muscolo scheletrico.

Materiali e Metodi: Le cellule AFS sono state ottenute mediante amniocentesi e selezionate per la positività al marcatore c-kit con metodo immmunomagnetico. Appena isolate le cellule AFS sono state analizzate per l'espressione di diversi marcatori (CD90, CD45, CD44, CD34, CD31, Flk1, SCA1, CD105) tramite citometria a flusso; inoltre, attraverso qRT-PCR è stata analizzata l'espressione di *Oct4*, *Sox2*, *c-Myc*, *Klf4* e *Sca-1* delle cellule AFS isolate a diversi stadi embrionali.

Per la terapia di topi transgenici *HSA-Cre, Smn*$^{F7/F7}$, le cellule AFS GFP+ sono state iniettate per via sistemica attraverso la vena caudale; gli animali sono stati poi sacrificati a uno e a quindici mesi dopo il trapianto. Sono stati osservati e analizzati alcuni parametri clinici per valutare l'effetto del trapianto cellulare. Diversi muscoli sono stati raccolti ed analizzati con ematossilina e eosina, tricromica di Masson e mediante immunofluorescenza con anticorpi anti-GFP e anti-distrofina. Per dimostrare la capacità delle cellule AFS di colonizzare la nicchia staminale del muscolo, sono state eseguite delle immunofluorescenze per i marcatori specifici delle cellule satelliti e sono stati eseguiti dei trapianti secondari. Il potenziale miogenico delle cellule AFS è stato valutato anche con trapianto dopo espansione *in vitro*.

Risultati: Il numero medio di cellule AFS presenti nel liquido amniotico varia nel corso della gestazione murina; all'età di 12.5 giorni queste cellule sono circa l'1% del totale ed esprimono marcatori ematopoietici (CD45, CD34, SCA1), marcatori mesenchimali (CD90, CD105) unitamente a Flk1, CD31 e CD44. L'analisi di espressione genica ha dimostrato che le cellule AFS esprimono a bassi livelli *Oct4* e *Sox2* e alti livelli di *c-Myc* e *Klf4*, mentre, nonostante la composizione mista di questa popolazione, non è stata rilevata espressione di marcatori o fattori di trascrizione tipici dei precursori muscolari.

I topi *HSA-Cre, Smn*$^{F7/F7}$ mediamente muoiono all'età di 10 mesi e durante il corso della loro vita mostrano evidenti complicazioni cliniche come una pronunciata cifosi e atrofia a livello muscolare. Dopo il trapianto con cellule AFS GFP+ o con cellule del midollo osseo, il tasso di sopravvivenza di questi animali aumenta rispettivamente del 75% e 50%. Gli animali trattati con cellule AFS hanno recuperato più del 75% della forza rispetto agli animali non trattati. Un mese dopo il trapianto, i muscoli di topi trattati con cellule AFS presentano il 37% di fibre GFP+, un numero molto basso di miofibre rigeneranti (< 1%) ed una normale espressione di distrofina. Quindici mesi dopo il trapianto, gli animali trattati con cellule del midollo osseo mostrano un elevato numero di fibre centro nucleate, un'importante infiltrazione di tessuto interstiziale e nessuna miofibra

GFP+, mentre i topi trattati con cellule AFS hanno un fenotipo molto simile a quello di topi sani della stessa età, e il 58% delle miofibre è GFP+. Risultati simili sono stati ottenuti trattando lo stesso modello animale con cellule AFS dopo espansione in cultura.

Discussione: Le cellule AFS isolate dal liquido amniotico di topo sono una popolazione eterogenea; queste cellule esprimono marcatori mesenchimali, ematopoietici e marcatori endoteliali. Va evidenziato che, nonostante la composizione mista di questa popolazione staminale, non esistono precursori muscolari al suo interno, e quindi qualunque differenziamento in senso muscolare di queste cellule è dovuto ad una differenziazione delle cellule AFS e non ad una maturazione di cellule già pre-commited.

Quando vengono iniettate in un modello di atrofia muscolare, le cellule AFS mostrano un grande potenziale miogenico, anche a lungo termine, dimostrandosi una interessante fonte cellulare per scopi terapeutici. Queste cellule infatti sono state in grado di differenziare in cellule satelliti localizzandosi nella nicchia delle cellule staminali muscolari ed esprimendo Pax7, α7integrina e SM/c-2.6, tutti marcatori esclusivi delle cellule satelliti. Inoltre, le cellule AFS possono contribuire alla formazione di nuove miofibre anche dopo espansione in cultura, aumentando così lo spettro di possibili applicazioni terapeutiche.

Parte del materiale prodotto nei tre anni di studio ha portato alla pubblicazione di un articolo scientifico:

Amniotic fluid stem cells restore the muscle cell niche in a HSA-Cre, Smn(F7/F7) mouse model.

Piccoli M, Franzin C, Bertin E, Urbani L, Blaauw B, Repele A, Taschin E, Cenedese A, Zanon GF, André-Schmutz I, Rosato A, Melki J, Cavazzana-Calvo M, Pozzobon M, De Coppi P.

Stem Cells. 2012 Aug;30(8):1675-84. doi: 10.1002/stem.1134.

ii. Abstract

Introduction: Stem cell biology has received much interest because of its potential in both therapeutic application and *in vitro* modeling of diseases. In particular embryonic stem cells have good proliferative and differentiative abilities, but their use is still associated to ethical concerns and problems related to their teratogenic potential. Adult stem cells have also been described to be pluripotent both *in vitro* and *in vivo*. However, their use is limited because they are difficult to isolate and expand, particularly in a clinical setting. In this scenario, it would be advantageous to obtain a cell population with high self-renewal and differentiation capacities, without ethical problems. In 2007 our group described that amniotic fluid stem (AFS) cells could be derived selecting amniocytes using c-Kit antibody. AFS cells have clonogenic capability and can be directed into a wide range of cell types representing the three primary embryonic lineages.

Aim: This work aiming at characterize the myogenic potential of mouse AFS cells using a mouse model of spinal muscular atrophy and in particular at analyzing their ability to differentiate into satellite cells and colonize the muscle stem cell niche.

Materials and Methods: Mouse AFS cells were obtained by amniocentesis and selected for the marker c-Kit with immunomagnetic beads. Freshly isolated AFS cells were analyzed for the expression of different markers (CD90, CD45, CD44, CD34, CD31, Flk1, SCA1, CD105) by flow cytometry and the expression of *Oct4*, *Sox2*, *c-Myc*, *Klf4* and *Sca-1* by qRT-PCR at different embryonic stages.

For the treatment of *HSA-Cre, Smn*$^{F7/F7}$ mutant mice, GFP+ AFS cells were injected via the tail vein and animals were sacrificed one and fifteen months after transplantation. Clinical aspects were observed and analyzed after

transplantation to evaluate AFS cells' effects. Several muscles were stained with hematoxylin and eosin, Masson's trichrome and analyzed by immunofluorescence with anti-GFP and anti-dystrophin antibodies. To demonstrate the ability of AFS cells to replenish the muscle niche, staining for satellite cell markers and secondary transplantation were performed. The myogenic potential of AFS cells was also evaluated with transplantation after *in vitro* expansion.

Results: Mouse AFS cell number changes during the course of gestation. At E12.5 these cells express hematopoietic markers (CD45, CD34, SCA1), mesenchymal markers (CD90, CD105) together with Flk1, CD31 and CD44. Gene expression analysis showed that mouse AFS cells express at low levels *Oct4* and *Sox2* and at high levels *c-Myc* and *Klf4*, whereas they are negative for the expression of myogenic genes.

Mild muscular mutant *HSA-Cre, Smn*$^{F7/F7}$ mice die at the age of 10 months and show evident clinical complications such as kyphosis and muscle shrinkage. After transplantation with GFP+ AFS or bone marrow (BM) cells mice survival rate increased by 75% and 50% respectively. Animals treated with AFS cells recovered more than 75% of force compared to the untreated. One month after transplantation, muscles obtained from AFS-treated mice displayed 37% of GFP+ fibers, with very low number of regenerating myofibers (<1%) and normal dystrophin expression. Fifteen months after transplantation BM-treated mice displayed a high number of central nucleated fibers and consistent infiltration of interstitial tissue and no GFP+ myofibers, while AFS-treated mice had a normalized phenotype, close to the same age WT mice, and 58% of the myofibers were GFP+. Similar results were obtained with transplantation of mouse AFS cells expanded in culture.

Discussion: Mouse AFS cells are a heterogeneous population, and their phenotype changes during the course of gestation. At E12.5 they express mesenchymal, hematopoietic and endothelial markers, but most importantly do

not express myogenic factors, indicating that no myogenic progenitor cells are present in this stem cell population.

When injected in a muscular mutant mouse model, AFS cells showed a myogenic potential, even after long-term transplantation, suggesting an interesting therapeutic potential. They indeed were able to differentiate into satellite cells localizing in the muscle stem cell niche and expressing Pax7, α7integrin and SM/c-2.6, exclusively markers of satellite cell population. Moreover, AFS cells could contribute to the formation of new myofibers even after *in vitro* expansion.

Part of the results described here produced a scientific paper:

Amniotic fluid stem cells restore the muscle cell niche in a HSA-Cre, Smn(F7/F7) mouse model.

Piccoli M, Franzin C, Bertin E, Urbani L, Blaauw B, Repele A, Taschin E, Cenedese A, Zanon GF, André-Schmutz I, Rosato A, Melki J, Cavazzana-Calvo M, Pozzobon M, De Coppi P.

Stem Cells. 2012 Aug;30(8):1675-84. doi: 10.1002/stem.1134.

iii. Introduction

Regenerative medicine has been receiving much attention in the last years because of possible benefits in clinical practice in both surgical and medical fields. The considerable development is mainly due to the discovery of cells with peculiar characteristics, described as stem cells, that possess both the capability of self-renewal and differentiation into organ-specific cell types. Different sources of stem cells have been identified in many adult mammalian tissues, such as bone marrow, skeletal muscle, skin and adipose tissue, where they contribute to the replenishment of cells lost due to normal cellular senescence or injury *(De Rosa and De Luca, 2012; Friedenstein et al., 1978; Mauro, 1961; Zuk et al., 2002)*. Mesenchymal stem cells, derived from whole bone marrow, have been shown to contribute to regenerating skeletal and cardiac muscle, bone, cartilage and also adipose tissues. However, their therapeutic potential is limited and, although stem cells in adult tissues may be capable of differentiating into more cell types than originally thought, they have a limited cellular regeneration or turnover *(Ferrari et al., 1998; Gussoni et al., 1999; Siegel et al., 2012)*.

In contrast, stem cells derived from embryonic sources have the ability not only to proliferate and replace themselves indefinitely, but have also the potential to form any cell type. Embryonic stem (ES) cells are derived from the inner cell mass of pre-implantation embryos, are pluripotent and demonstrate germ-line transmission in experimentally produced chimeras. Other important characteristics include growth as multicellular colonies, normal and stable karyotypes, ability to be continuously passaged and the capability to differentiate into cells of all the three embryonic germ layers (**Figure 1**). Although there is great interest in ES cell research, the use of embryos to harvest cells is still associated with unresolved ethical concerns. Moreover, ES cells from some species can form teratocarcinomas when injected into histocompatible or immunologically compromised mice. Finally, immunological reactions are

normally associated to their transplantation because of the different genetic profile between donor and recipient *(Grinnemo et al., 2008).*

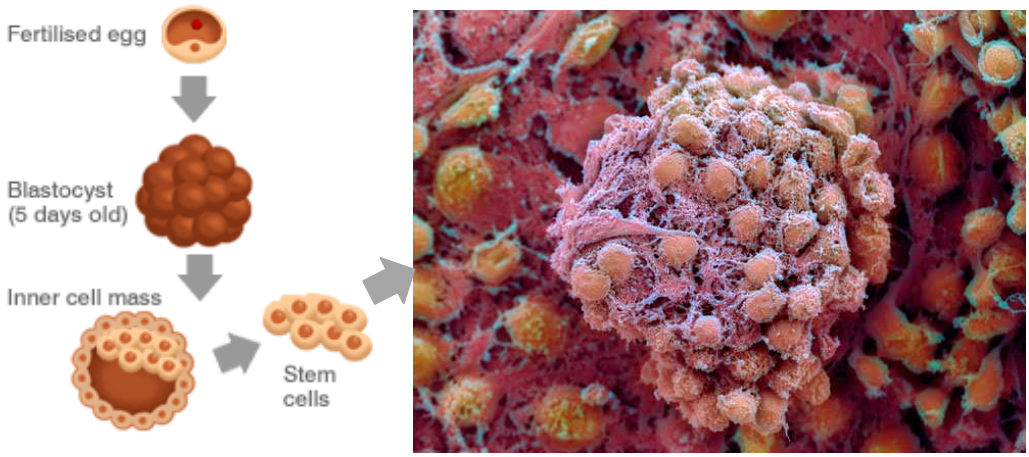

Figure 1. Embryonic stem cells. From the zygote to the blastocyst before implantation. ES cells are isolated from the inner cell mass and when put in culture growth as multicellular colonies.

In order to overcome problem related to both ethical and immunological issues, an alternative approach has been recently shown. Both murine and human fibroblasts have been reprogrammed directly to pluripotency by ectopic expression of four transcription factors (*Oct4, Sox2, Klf4* and *Myc*) to yield induced pluripotent stem (iPS) cells *(Takahashi and Yamanaka, 2006; Yamanaka, 2010)*. They can be derived from adult human fibroblast and it could be possible to envisage in the next future that they could be used for autologous application without any rejection problem. Human iPS cells resemble ES cells in morphology, gene expression and the capacity to form teratomas in immune-deficient mice. However, clinical success with human iPS cells is still far to come and must await the development of methods that avoid both potentially harmful genetic modification and problems related to their teratogenic potential.

1. Amniotic fluid stem cells

For all those reasons many groups are still focusing on different stem cell populations for therapeutic applications. Fetal tissue has been used for autograft and allograft transplantation because of its proliferative ability and lack of immunogenicity. Fetal tissue can be currently obtained from a biopsy or from cord blood sampling of the fetus itself during gestation; however, both procedures are associated with a defined morbidity. Fetal tissue can also be obtained from aborted embryos, but this resource is limited. Amniocentesis is a well established technique for the collection of fluid from the human fetus during pregnancy (12 weeks to term). Cultured cells from amniotic fluid are widely used for the prenatal diagnosis of genetic disorders. The morphologic heterogeneity of these cells is well known and different criteria have been used for their characterization *(In 't Anker et al., 2003)*. We have described that pluripotent stem cells can be isolated from amniotic fluid, defined as amniotic fluid stem (AFS) cells by selection for the expression of the membrane stem cell factor receptor c-Kit (CD117), a common marker for multipotent stem cell *(De Coppi et al., 2007a)* (**Figure 2**). These cells have a high renewal capacity and can be expanded for over 250 doublings without any detectable loss of chromosomal telomere length. We have described their potential to give rise, *in vitro,* to adipocytes-, hepatocytes- and endothelial-like cells, and, *in vivo*, to differentiate towards neurogenic and osteogenic lineages. Furthermore, AFS cells could be differentiate towards cardiomyogenic lineages, when co-cultured with neonatal cardiomyocytes *(Bollini et al., 2010; Chiavegato et al., 2007)*, or hematopoietic lineage when transplanted into immuecompromised $Rag1^{-/-}$ mice *(Ditadi et al., 2009)*. Moreover, rat AFS cells have been able to improve the repair of the damaged smooth muscle in a cryoinjured bladder *(De Coppi et al., 2007b)* and the clinical appearance and intestine function when injected in a rat model of necrotizing enterocolitis *(Zani et al., 2013)*.

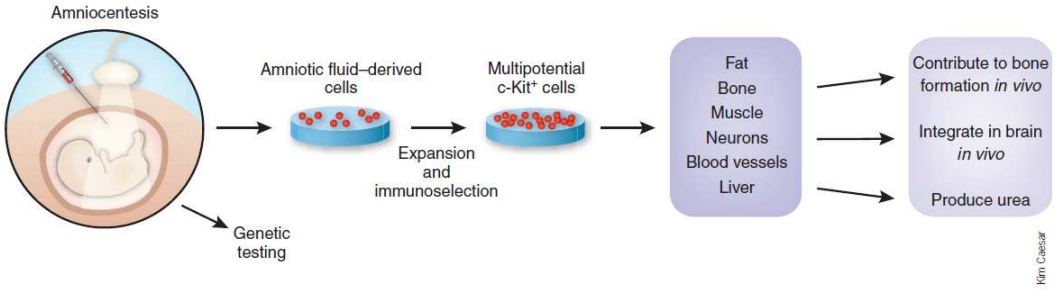

Figure 2. Amniotic fluid stem cells. Multipotent AFS cells are isolated by collecting a heterogeneous population of cells through amniocentesis and selecting cells that express c-Kit. Under appropriate inducing conditions, the c-Kit+ cells can be differentiated into cell of all three primary germ layers.

2. Spinal muscular atrophy mouse model

In order to test the hypothesis that AFS cells could functionally engraft also in a diseased skeletal muscle, we used a mouse model of spinal muscular atrophy (SMA), in which the phenotypic disease is full blown in muscle tissue *(Nicole et al., 2003)*.

Spinal muscular atrophy is an autosomal recessive disorder that affects the spinal cord neurons, and is clinically characterized by muscle weakness and genetically by mutations in the survival motor neuron (*SMN*) gene. Children with SMA experience weakness over a wide range of severity. Type 1 SMA patients are never able to sit independently and generally die in infancy. Type 2 SMA can sit but often develop severe pulmonary and orthopedic complications, and type 3 SMA children acquire the ability to walk although this might be lost during the course of the disease. In all forms of SMA the most rapid rate of decline is early in the course of the disease, with a progressively slower rate of decline over the time, and sometimes years are needed to appreciate any further deterioration (*Crawford, 2004*). At the present, no effective therapy is available for SMA, besides supportive care. Consequently, the development of novel therapies in SMA now has strong academic, government, and industry involvement, in addition to the interest of several parental organizations and foundations.

There are normally two copies of *SMN* gene on each chromosome, the primary gene copy called *SMN1*, and almost an identical copy, *SMN2*. Loss of *SMN1* is essential to the pathogenesis of SMA, while the severity of the disease is primarily related to the number of copies of *SMN2*. In contrast to the human, the mouse *Smn* gene is not duplicated, which may explain the fact that the conventional knockout of the *SMN* gene results in embryonic lethality (DiDonato et al., 1997; Schrank et al., 1997; Viollet et al., 1997).

In our mouse model, the murine *Smn* exon 7 (the most affected exon in human SMA) is flanked by two LoxP sequences (Smn^{F7}) and deletion is occurring only in skeletal myofibers by placing the Cre recombinase under the control of the a-skeletal actin gene promoter (*HSA-Cre*). Similarly to other models of muscle disease, *HSA-Cre,* $Smn^{F7/F7}$ mice display a high proportion of myofibers with central nuclei, which lead with time to muscle fibers necrosis, heterogeneous myofiber diameters, and infiltration of interstitial tissue *(Nicole et al., 2003)*. *HSA-Cre,* $Smn^{F7/F7}$ animals manifest kyphosis, progressive muscle weakness, shrinkage, and subsequent respiratory arrest, similarly to the clinical features exhibited by the dystrophic *mdx/mTR* mouse model *(Sacco et al., 2010)*. Therefore, the overall survival of *HSA-Cre,* $Smn^{F7/F7}$ animals is estimated to be of 10 months. It has been shown that after bone marrow (BM) transplantation, the myopathic phenotype attenuates and myofibers number and motor performance normalize up to 9 months of age *(Salah-Mohellibi et al., 2006)*. However, the engraftment in the diseased muscle tissue is poor: the cells are not able to rescue the phenotype and make a substantial, long-term therapeutic contribution *(Salah-Mohellibi et al., 2006)*.

iv. Aim

Since the total absence of potential therapies to treat SMA disorder, the development of novel therapies in SMA has strong interest.

The aim of this work was to establish whether AFS cells transplantation would produce physiologically and functionally significant skeletal muscle repair in the *HSA-Cre, Smn*$^{F7/F7}$ mouse model, with integration in the muscle niche and differentiation into satellite cells.

vi. Materials and Methods

1. Mice

Male C57BL/6 (Ly5.2) GFP+/-mice and female C57BL/6 (Ly5.2) GFP-/- mice were used to obtain both Ly5.2 GFP+/- and GFP-/- embryos. *HSA-Cre, Smn*$^{F7/F7}$ mice were used as recipients. All procedures were approved by the University of Padua's Animal Care and Use Committee (CEASA, protocol references 107/07 and 41056) and, in accordance with Italian law, were communicated to the Ministry of Health and local authorities.

2. Amniotic fluid collection and stem cell selection

Embryo age was defined relative to the morning of vaginal plug discovery (E0.5). All dissections were performed under a stereomicroscope (Leica Microsystems). Amniotic fluid samples were harvested from pregnant mice at E12.5. Amniocentesis has been done following an accurate procedure: first there was the removal of maternal uterine wall, to expose the yolk sac. At this point the chorion and yolk sac were carefully removed. Amnion rupture resulted in amniotic fluid leakage, and amniotic fluid was harvested with a syringe fitted with a 28-gauge needle. Mouse amniotic fluid-derived c-Kit+ cells were isolated using the Miltenyi Mouse Lineage Cell depletion kit and the CD117 MicroBeads kit (all from Miltenyi Biotech).

3. Flow cytometry analysis

Flow cytometry was performed using a FACSCalibur flow cytometer (BD Biosciences) with CellQuest acquisition software (BD Biosciences). The antibodies used were CD177 APC (Biolegend) or CD117 PE Cy5 (eBioscience), Sca1 FITC, CD90 FITC, CD44 FITC, CD45 PE and CD105 PE (All from BD Biosciences), and the 7AAD (BD pharmingen) as viability probe.

4. Bone marrow collection

Wild-type (WT) BM cells were isolated under sterile conditions from 6- to 10-week-old isogenic mice that ubiquitously expressed green fluorescent protein (GFP). The femur and tibia were surgically removed and placed in Dulbecco's modified Eagle's medium (DMEM) culture medium with 10% fetal bovine serum (FBS) (Gibco). Marrow was collected and red blood cells were lysed with 0.75% NH4Cl in 20 mM Tris, pH 7.2.

5. Fetal liver cells isolation and selection

Fetal liver samples from GFP+ embryos were harvested between embryonic days E11.5 and E13.5, as described for amniotic fluid. After mechanical disaggregation, murine fetal liver c-kit+ cells were isolated using the Miltenyi Mouse Lineage Cell depletion kit and then CD117 MicroBeads using the same protocol validated with AFS cells.

6. AFS cell expansion

Freshly isolated GFP+ AFS cells were plated onto a feeder layer of mitomycin C-treated mouse embryonic fibroblasts SNL (applied Stem Cells Inc.) in DMEM knockout (Invitrogen) supplemented with 15% heat-inactivated FBS (Invitrogen), 0.1 mM nonessential aminoacids (Invitrogen), 2 mM L-glutamine (Invitrogen), 50 U (ug)/ml penicillin/streptomycin (Invitrogen), 0.01 mM 2-mercaptoethanol (Sigma), 10 ng/ml BMP4 (R&D Systems), and 20 ng/ml LIF (Sigma). Cells were cultivated at 37°C and 5% CO2.

7. Cell injection

Three-month-old *HSA-Cre,Smn*$^{F7/F7}$ mice were randomized to receive either no treatment, mouse BM cells, or mouse AFS cells. Approximately 25,000 GFP+ cells were injected via tail vein in the AFS cells group and 50,000 GFP+ cells were injected via tail vein in the BM group. *In vitro* expanded AFS cells were sorted

with an Aria FACS system (Becton Dickinson) and selected for the expression of GFP and c-kit prior to injection. After sacrifice at 1 month post-transplantation (pt), muscle differentiation and regeneration were investigated by assessing the percentage of cells derived from donor GFP+ cells in recipient muscles, considering the total number of muscle fibers (both centrally nucleated and with peripheral nuclei).

8. Secondary transplants

Single myofibers were isolated from BM- and AFS-transplanted animals and from C57BL/6 GFP+/- mice, as previously described *(Rossi et al., 2011)*. Briefly, *extensor digitorum longus* (EDL) and *Soleus* muscles were digested for 2 hours at 37C in 0.2% (wt/vol) type I collagenase (Sigma-Aldrich), reconstituted in DMEM (high glucose, with L-glutamine, supplemented with 1% penicillin-streptomycin; Invitrogen). Following digestion, muscles were transferred in DMEM (low glucose; Invitrogen) on a horse serum (Invitrogen)-coated 10-cm dish (Falcon; BD Biosciences) and gently triturated with a wide-bore pipette to release single myofibers. Fresh satellite cells (SCs) were stripped off the fibers by repeated passage through an 18-gauge needle. Five hundred cells were injected locally into *tibialis anterior* (TA) of naive, 3-month-old *HSA-Cre, Smn*$^{F7/F7}$ mice. Animals were sacrificed at 1 month pt.

9. In vivo imaging

Prior to imaging, mice were anesthetized (with a mixture of Rompum and Zoletil given i.p.), shaved and depilated to completely remove hair, and imaged on the eXplore Optix time-domain imager (ART, Montreal, Quebec). Image processing and data analysis were performed using explore Optiview 1.04 software (ART).

10. Muscle physiology, histology, and immunofluorescence analyses

In vivo determination of *gastrocnemius* strength and contraction kinetics was carried out as described previously *(Blaauw et al., 2008)*. Transverse sections (8–10 μm thick) of isopentane-frozen skeletal muscle (TA) of 3-month-old transplanted mice were stained with hematoxylin and eosin and Masson's trichrome. To evaluate the total number of centrally nucleated muscle fibers, serial 40 μm sections of the entire TA muscle were prepared. Immunostaining of GFP or dystrophin was performed using rabbit anti-GFP (1:200; Invitrogen) or anti-dystrophin (1:150; Abcam). Sections were mounted with Vecta-shield and 4,6-diamidino-2-phenylindole (Vector Laboratories), observed under an Olympus BX60 microscope (Olympus), and pictures taken using Viewfinder Lite software.

11. Image processing

A total of 38 images related to 6 types of muscle fibers were analyzed to highlight the different fiber dimension distribution through a quantitative evaluation. To this aim, for each image, fibers have been segmented and their boundaries analytically obtained by using an automatic procedure and tuned for the specific case study. Then, the shape data have been collected from each group and the area computation has been performed numerically, and finally summarized with mean and variance (due to the high number of samples).

12. Western blot

Frozen skeletal muscles (TA of affected mice (n=2), TA of AFS- (n=4) and BM- (n=4) treated mice 1 month pt and TA of AFS- (n=2), BM- (n=2) 15 months pt) were crashed with mortar and pestle in liquid nitrogen and transferred in RIPA buffer with protease inhibitor cocktail (Sigma). Anti rabbit GFP (1:700, Invitrogen) and anti mouse Actinin (1:5000, Sigma) were used.

13. RNA extraction and Real Time PCR

Total RNA has been extracted from freshly isolated AFS cells or muscle samples using RNeasy Plus Mini kit (QIAGEN GmbH) following the supplier's instructions.

RNA has been then quantified with a ND-1000 spectrophotometer (Thermo Scientific) and 1 μg has been retrotranscripted with SuperScript II and related products (all from Invitrogen) in a 20 μl reaction. Real-time PCR (qRT-PCR) reactions were performed using a LightCycler II (Roche). Reactions have been carried out in triplicate using 4 μl of FASTSTART SYBR GREEN MASTER (Roche) and 2 μl of primers mix FW plus REV (final concentration, 300/300 nM) in a final volume of 20 μl. Serial dilutions of a positive control sample have been used to create a standard curve for the relative quantification. The amount of each mRNA has been normalized for the content in *β2-microglobulin*. Primer sequences are listed in **Table 1**.

14. DNA extraction and PCR analyses

DNA from organ and tissues samples was extracted with a DNeasy Blood & Tissue kit (QIAGEN GmbH) and then quantified with a ND-1000 spectrophotometer (Thermo Scientific). Genomic DNA samples extracted from GFP+ AFS cells and from WT organs were, used respectively as positive and negative controls for the amplification of the GFP gene. PCR reactions for the TERT and GFP genes were carried out as previously described *(Ghionzoli et al., 2009)*. Primers sequences listed in **Table 1**.

15. Statistical analyses

Values were reported as means ± SD or SE. Statistical significance of the differences between means were assessed by analysis of variance followed by the Student−Newman−Keuls test or by Student's t−test for paired or nonpaired data. Statistical significance was set at $P< 0.05$.

Table 1. Primers list.

Name	Forward 5' >3'	Reverse 5' >3'
c-kit	TGGTCCGCTGCCCTCTGACA	CCTTGATGGCTGCCCGCACT
Oct4	TGGAGGAAGCCGACAACAATGAGA	TGGCGATGTGAGTGATCTGCTGTA
Nanog	CCCTTCCCTCGCCATCACACTG	GGAAGGGCGAGGAGAGGCAGC
Sox2	TCGGGGAAGCGTGTACTTAT	CATGCACAACTCGGAGATCA
Klf4	TGCCCCGACTAACCGTTGGCGT	GCTGCACCAGCTCCGCCACT
c-Myc	TGCCCGCGATCAGCTCTCCT	CGTGGCTGTCTGCGGGGTTT
Pax7	AGCAAGCCCAGACAGGTGGCG	GGCACCGTGCTTCGGTCGCA
Myf5	ACAGCAGCTTTGACAGCATC	AAGCAATCCAAGCTGGACAC
Mrf4	GGCTGGATCAGCAAGAGAAG	AAGAAAGGCGCTGAAGACTG
MyoD	CGCTCCAACTGCTCTGATG	TAGTAGGCGGTGTCGTAGCC
Myogenin	GCAATGCACTGGAGTTCG	ACGATGGACGTAAGGGAGTG
β2microgl.	GCTTCAGTCGTCAGCATGG	CAGTTCAGTATGTTCGGCTTCC
GFP	TGAACCGCATCGAGCTGAAGGG	TCCAGCAGGACCATGTGATCGC
TERT	ACCCACTATCCTTGTGGTGCATGA	AGATCGAGCAGCTGCAAGACCATA

vi. Results

1. Mouse AFS cell characterization

Mouse amniotic fluid was collected from offspring of GFP-/- female and GFP+/- males, and all the analyses were performed on cells selected for GFP expression to avoid any maternal contamination (**Figure 3A**). A lineage depletion for hematopoietic lineage was done on the collected amniotic fluid, to remove all the mature cells, and after that a selection for the marker c-Kit was carried out. About 1% c-Kit positive cells were detected among all amniotic fluid cells isolated at E12.5, and the total number of mouse AFS cells per embryo equivalent was around 16.000 cells (**Figure 3B**).

As mentioned before, human AFS cells were characterized for their expression of pluripotency markers like Oct4 and SSEA4. Mouse AFS cells were indeed studied for the expression of the pluripotency markers *Oct4*, *Sox2*, *Nanog*, *c-Myc* and *Klf4*. Real Time-PCR analysis showed that the expression of these markers was very low if compared with that of mouse ES cells, and importantly, mouse AFS cells did not express *Nanog* (**Figure 3C**).

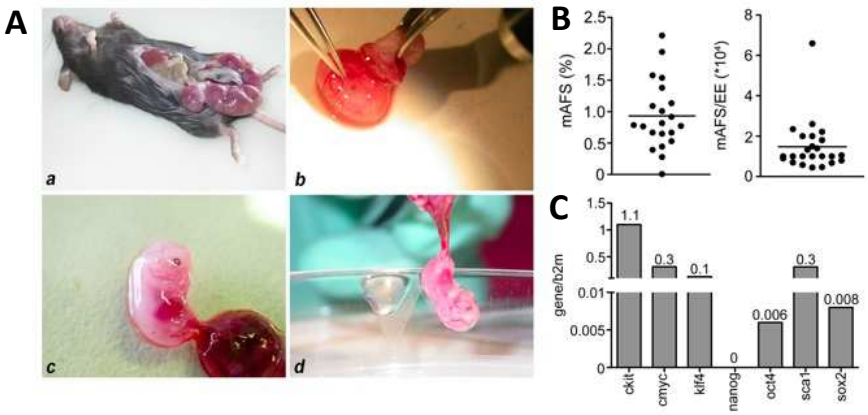

Figure 3: Presence of mouse AFS cells in the mouse amniotic fluid. (A) Mouse amniotic fluid collection. **(B)** Left panel: percentage of mouse AFS cells at E12.5. Right panel: total number of mouse AFS cells per embryo equivalent (EE). Means are represented by bars. **(C)** Gene expression profile of AFS cells collected at E12.5.

An immunophenotype analysis was performed to characterize E12.5 mouse AFS cells: they express characteristic markers of hematopoietic (CD45, CD34, Sca1) and mesenchymal (CD90, CD105) stem cells together with CD44, CD31 and Flk1 (**Figure 4**). Considering the c-Kit+ sub-population, CD90 was expressed by 30% of cells; CD45, a marker that define the commitment to the hematopoietic lineage, was expressed by 32% of cells; CD31 (platelet endothelial cell adhesion molecule 1, Pecam-1) is a marker expressed by endothelial cells, and its expression in the c-Kit+ cells ranged from 12 to 25%. CD34, a hematopoietic stem cells marker, is expressed by 20% of cells. Flk1, the receptor for vascular endothelial growth factor (VEGFR), changed consistently among all the analyzed sample, indeed it was expressed from 5% to 50% of AFS cells isolated at E12.5; Sca1, a characteristic marker of hematopoietic stem cells and other adult stem cells, was expressed by 20% of the cells. CD105 is another marker of mesenchymal stem cells, and it was expressed by 40% of the c-Kit+ cells; CD44 is a cell surface glycoprotein involved in cell-cell interactions, and in the amniotic fluid was expressed by more than 50% of c-Kit+ cells.

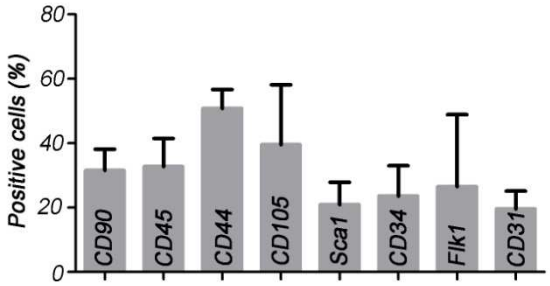

CD90	31.8 ± 6.32	Sca1	20.96 ± 9.79
CD45	32.78 ± 12.32	CD34	23.64 ± 13.32
CD44	50.82 ± 8.34	Flk1	26.59 ± 31.57
CD105	39.59 ± 26.33	CD31	19.66 ± 7.79

Figure 4: Phenotypic characterization of E12.5 mouse AFS cells. Mouse AFS cells were stained with antibodies specific for CD90, CD45, CD31, CD34, Flk1, Sca1, CD105 and CD44. The histograms show expression of the markers and the table shows percentage of expression with mean and s.d.

Since the heterogeneity of AFS cells, we performed a myogenic expression profile to exclude the presence of muscle precursor cells in the c-Kit positive selected population. As shown in **Figure 5**, we didn't find expression of either early or late myogenic specific genes.

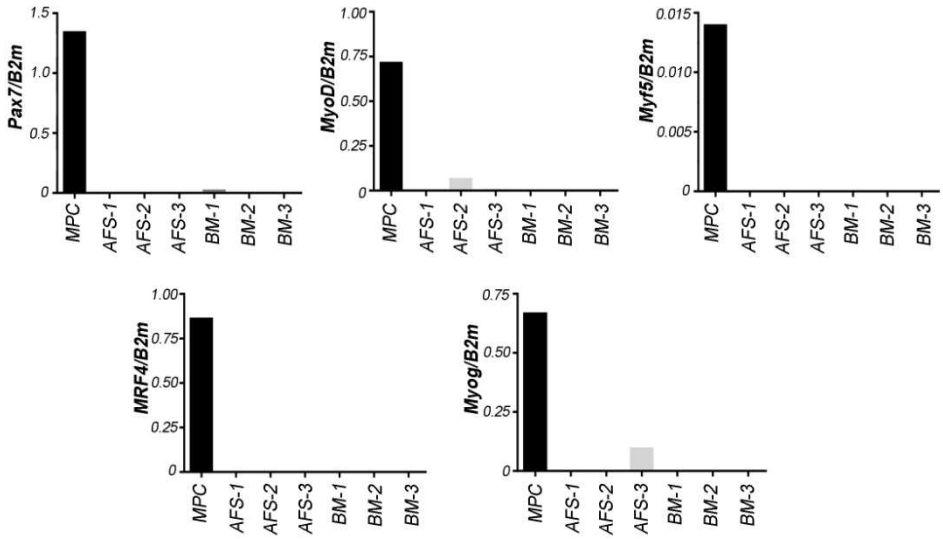

Figure 5: Expression of myogenic genes. Three sample of mouse AFS cells and BM cells were freshly isolated and analyzed for the expression of specific myogenic genes to exclude the presence of myogenic precursor cells among all the selected cells. Muscle precursor cells (MPC) were used as positive control.

2. AFS cell transplantation in mild muscular atrophy mouse model

At the age of 3 months, mutant mice (*HSA-Cre, Smn*$^{F7/F7}$) were randomized to receive via tail vein GFP+ AFS cells (25,000 cells, n=40), GFP+ BM cells (50,000 cells, n=20), or no treatment (untreated, n=20). AFS cells were derived and characterized as previously described. As expected, all untreated animals died by the age of 10 months, whereas the BM- and AFS-treated groups had at that time survival rates of 50% and 75% ($p < 0.001$), respectively (**Figure 6A**). The treated mice dramatically differed from the untreated animals: *gastrocnemius* contraction kinetics was measured blinded 1 month pt and this analysis

confirmed that both BM- and AFS-treated mice achieved strength levels comparable to the ones obtained with WT mice (**Figure 6B**). Remarkably, the AFS-treated animals, which survived until 15 months pt (i.e., 18 months of age), maintained the strength acquired at 1 month pt (**Figure 6B**). Consistently with survival and muscle strength, AFS-treated mice were similar to WT mice in terms of diaphragm thickness, weight, movement, and skeletal anatomy as confirmed at MicroCT scan analysis (**Figure 6C-F**). On the contrary, *HSA-Cre,Smn*$^{F7/F7}$, which did not receive any treatment, showed typical thinner diseased diaphragmatic muscles at 4 months of age (**Figure 6C**) and pronounced kyphosis with impaired movements by the age of 8 months (**Figure 6D-F**).

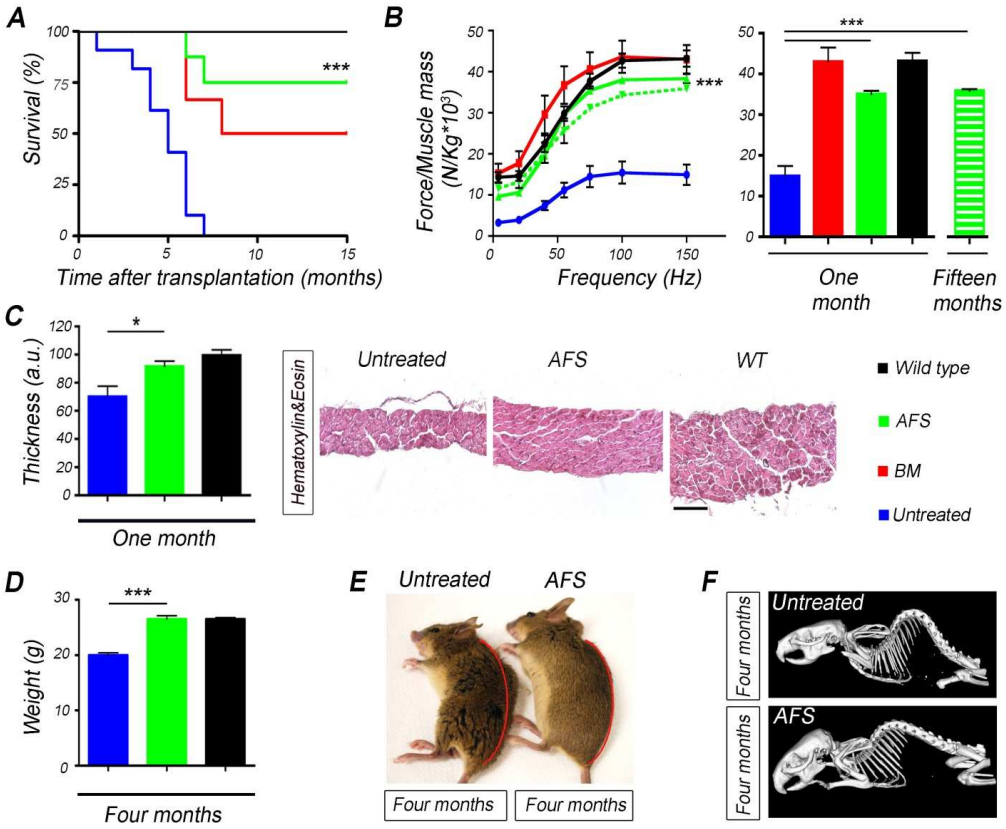

Figure 6: Transplanted animals improve in survival and clinical parameter. (A) Survival curve: AFS-treated mice increased life expectancy both when compared to BM-treated and untreated animals. Untreated=10 animals, BM=8 animals, AFS=8 animals (***p<0.001). **(B)** Left panel: muscle strength analyzed at different frequencies; right panel: mean value of muscle strength analyzed at 150 Hz of frequency. Normalized force frequency on muscle mass displays that both BM- (n=8) and AFS-treated (n=8) mice had 75% more muscle strength than untreated (n=6) animals one month after transplantation (***p<0.001). AFS-treated animals analyzed at 18

months of age (Green dotted line; n=4). **(C)** Diaphragm thickness one month after transplantation (n=3/group), in AFS-treated animals did not differed from age-matched WT animals while they are both distinct from untreated animals (scale bar =100 µm; *p<0.05). **(D)** Bodyweight of untreated (n=4), AFS-treated (n=4) and WT (n=8) mice at 8 months (***p<0.001). **(E)** The kyphosis, which is present in the untreated mice from 3 months of age, disappeared in AFS-treated mice. **(F)** MicroCT scan of skeletal anatomy of untreated and AFS-treated mice confirmed the different curvature of the spine.

When fiber diameter was measured, at first both AFS- and BM-treated muscles demonstrated a normalization of dimensions close to WT muscle; notably in the long-term experiments this normalization was maintained only by the AFS-treated muscles, while those treated with BM had very large hypertrophic fibers (**Figure 7**).

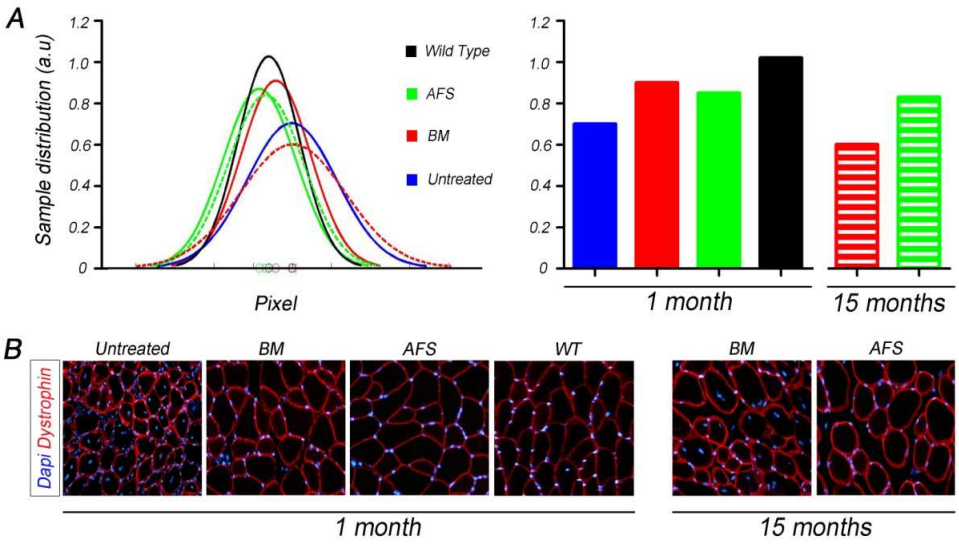

Figure 7: Stem cells-treated fibers diameter. (A) Distribution of fiber areas in WT (black), AFS-treated (green), BM-treated (red) and untreated (blu) muscles, 1 month and 15 months (dotted lines) after transplantation. **(B)** Example of dystrophin expression in all the analyzed samples.

3. Restoration of muscle phenotype after AFS cell transplantation

Following morphological muscle analyses performed 1 month pt (i.e., 4 months of age; **Figure 8A**), in both BM- and AFS-treated mice, the histological aspect of the muscle tissue resulted indistinguishable from WT, with few central nucleated fibers (<1%, comparable to WT mice; **Figure 8B, 8F, 8G**). In contrast, untreated animals presented a very large number of central nucleated fibers (mean value: 63.70% ± 0.41%, $p < 0.001$ vs WT; **Figure 8B, 8F, 8G**). Masson's trichrome staining showed that untreated animals presented large connective tissue areas between fibers, which were absent in both WT and cell-treated mice. Immunofluorescence analyses clearly indicated that the morphological appearance of muscle in BM- and AFS-treated animals was correlated with a relevant proportion of GFP+ fibers (31.57% ± 7.04% and 37.86% ± 9.48%, respectively; **Figure 8G**).

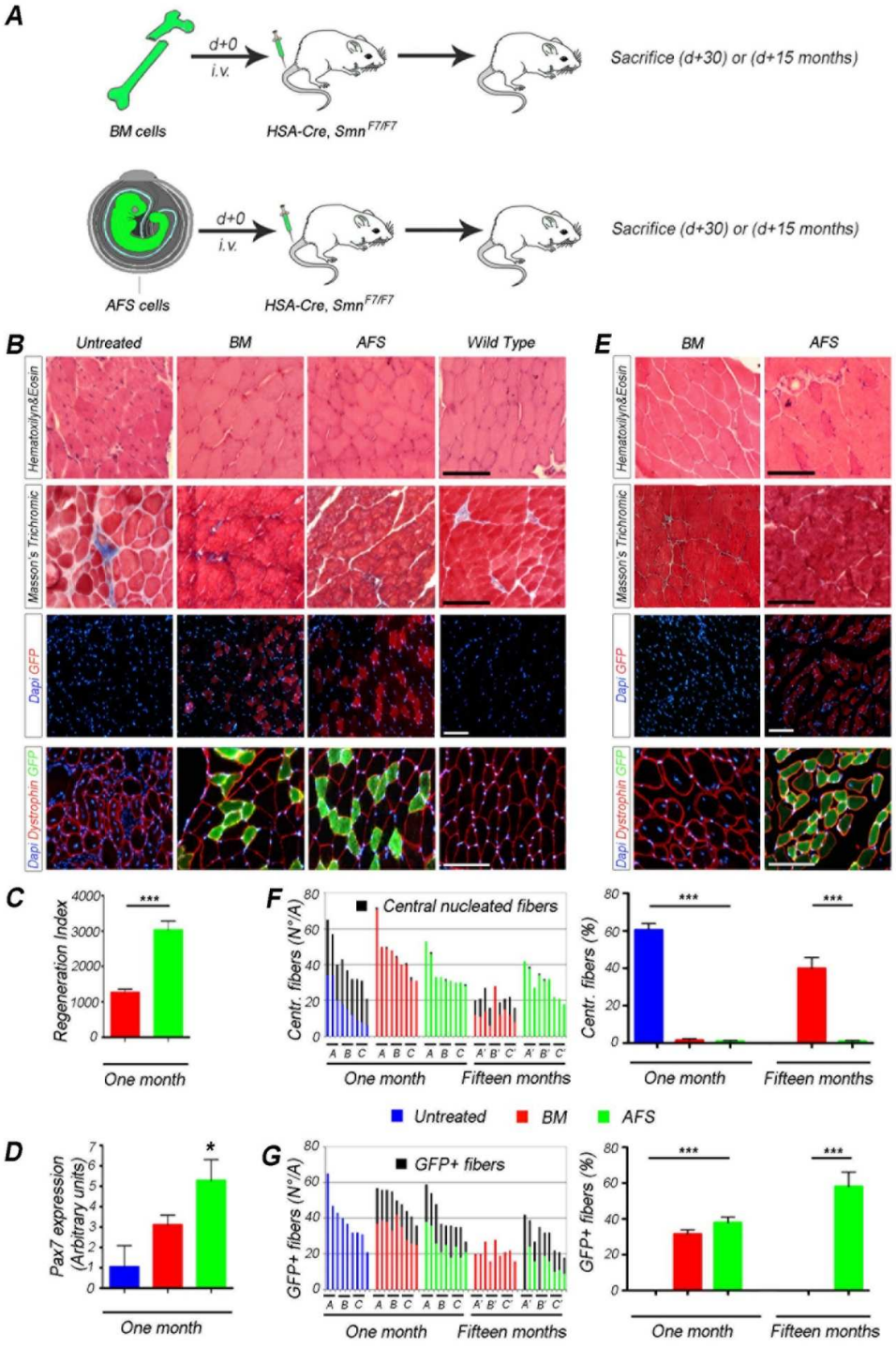

Figure 8: Restoration of muscle phenotype in mutant mice. (A) Three-month-old *HSA-Cre, Smn$^{F7/F7}$* mice were transplanted alternatively with BM or AFS cells and sacrificed 1 month after treatment for analyses. **(B)** One month after transplantation, H&E staining reveal a normal appearance of the TA muscle structure after receiving either BM or AFS cells. On the contrary TA muscle of untreated animals present fibers disarrangement (dystrophin staining) with interstitial tissue deposition identified at Masson's trichrome. Scale bar=100 µm. **(C)** Regeneration index indicates that AFS cells are more likely to participate in muscle regeneration than BM cells;***p<0.001. **(D)** qRT-PCR for Pax7 expression revealed that mutant muscles receiving AFS

cells (n=3) expressed higher levels of Pax7 than untreated (n=3) and BM (n=3) animals; *p<0,05. **(E)** Fifteen months after transplantation, histological and immunofluorescence analyses revealed a more sustained, long-term engraftment of AFS cells, relative to BM cells. Scale bar =100 µm. **(F-G)** Graphs of raw numbers (each letter on the x axis is an individual muscle evaluated in 3 representative high power fields) and percentages of centrally nucleated and GFP+ fibers on total number of fibers/area.

It is worth of notice that in this particular muscular model, the beneficial effect of AFS cells transplantation is detectable very soon after injection. In fact, only 12 hours after injection the number of centrally nucleated fiber greatly diminished (7.90% ± 2.31%) to look similar to WT muscle only after 7 days (0.53% ± 0.09%). Importantly, as shown before, this *in vivo* effect did not relate to the presence of myogenic precursors in the transplanted populations, which was excluded by demonstrating that the myogenic genes *Pax7*, *MyoD*, *Myf5*, *Mrf4*, and *Myogenin* were neither expressed in freshly isolated BM nor in AFS cells (**Figure 5**). Last, massive changes in the muscle tissue were also confirmed by the observed distribution of dystrophin expression, which was similar in transplanted mice compared to WT but was altered in the untreated animals (**Figure 8B**). It was not possible to consider the restoring of the Smn protein as amelioration in the transplanted animals since Smn is expressed also in the *HSA-Cre, Smn$^{F7/F7}$* mice (*Nicole et al., 2003*). Despite the similarity between BM- and AFS-treated animals in terms of physiology and number of central nucleated and GFP+ myofibers, the engraftment index, defined as the number of donor-engrafted myofibers generated per 10^5 transplanted cells (*Carraro et al., 2008*), differed significantly between BM- (1,263.00 ± 282.76) and AFS-treated mice (3,029.16 ± 758.71; $p < 0.001$), respectively (**Figure 8C**). Additionally, qRT-PCR revealed that 1 month after treatment, in the TA muscles of AFS-treated mice, there was higher expression of *Pax7* than in untreated or BM-treated mice ($p < 0.05$; **Figure 8D**). Further evidence of the differences between the two groups was confirmed by analysis of surviving animals 15 months pt (**Figure 8A**). Morphological analysis of samples from BM-treated mice displayed a high number of central nucleated fibers (39.90% ± 17.68%) and consistent infiltration of interstitial tissue between

the myofibers — a situation that differed greatly from the one observed in AFS-treated mice, where tissue appeared healthy and compact (**Figure 8E-8G**). Moreover, at this stage (15 months pt), no GFP+ fibers were found in BM-treated animals, whereas 58.00% ± 2.43% of myofibers were GFP+ in AFS-treated mice (**Figure 8E-8G**). This finding highlights the sustained effect of AFS cells transplantation. PCR analyses of genomic GFP performed 1 and 15 months pt proved that the AFS cells were able to engraft systemically throughout various skeletal muscles (**Figure 9A**) and this was also confirmed after Western blot performed in muscle samples (**Figure 9B**). The ability of AFS cells to engraft various skeletal muscle tissues was also validated by the fact that both the number of central nucleated and GFP+ fibers were comparable among *gastrocnemius*, EDL, and diaphragm at 1 month pt, with GFP+ fibers variation from 17.28% ± 3.66% for diaphragm to 38.52% ± 6.87% for EDL (**Figure 9C**). Moreover, this could also be explained by the migratory potential of AFS cells that is consistent, besides the skeletal muscle territory, with the multiple organ engraftment similar to the one observed after systemic injection of human AFS cells (*Carraro et al., 2008*) (**Figure 9D**).

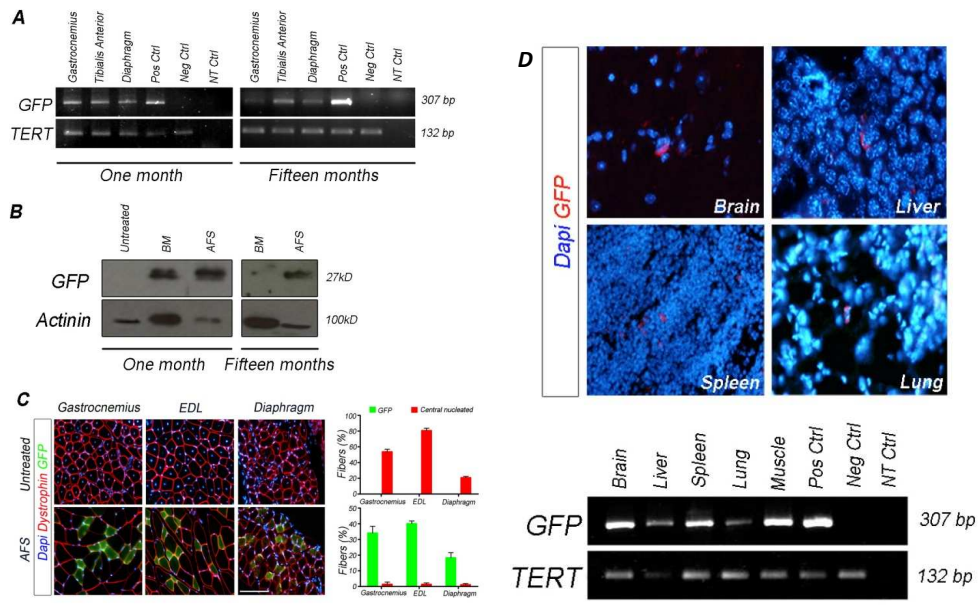

Figure 9: AFS cells distribution after tail vein injection. (A) PCR analyses of gastrocnemius, TA and diaphragm muscles isolated from AFS-treated mice one and fifteen months after

transplantation. First lane: amplification of the GFP gene (307 bp) in AFS-treated *HSA-Cre, Smn*$^{F7/F7}$ mice. Second lane: amplification of genomic TERT (132 bp) to confirm the quality of the extracted DNA. **(B)** Western blot analysis for GFP detection of TA muscles from untreated, BM- and AFS-treated mice obtained 1 month pt and from BM- and AFS-treated animals sacrificed 15 months pt. Actinin was used to confirm the quality of protein extraction. **(C)** Immunofuorescence analysis of gastrocnemius, EDL and diaphragm obtained from untreated and AFS-treated mice one month after transplantation and relative percentage of GFP+ and central nucleated myofibers. Scale bar =100 µm. **(D)** Immunofluorescence analyses with anti-GFP antibody in the brain, liver, spleen and lung of AFS-treated mice showed minimal systemic engraftment. The same and other organs were analyzed by PCR, first lane: amplification of the GFP gene; second lane: amplification of genomic TERT to confirm the quality of the extracted DNA. The positive control (Pos Ctrl) for GFP amplification was the genomic DNA extracted from GFP+ AFS cells; the negative (Neg Ctrl) was a TA of WT mouse; NT Ctrl=no template control; Muscle: lysate of gastrocnemius, TA and EDL treated muscles.

4. AFS cells engraft in the muscle stem cell niche and express satellite cell markers

Since AFS cells were able to sustain long-term muscle regeneration, we assumed that they were able to integrate into the muscle stem cell niche. In AFS-treated muscles, GFP+ cells were found in sublaminal position, and this observation was evident also when fibers were isolated in culture (**Figure 10A, 10B**). Moreover, some of these cells co-stained for Pax7 and alpha7integrin (α7int) both when adherent to the fiber and after stripping (**Figure 10C-E**).

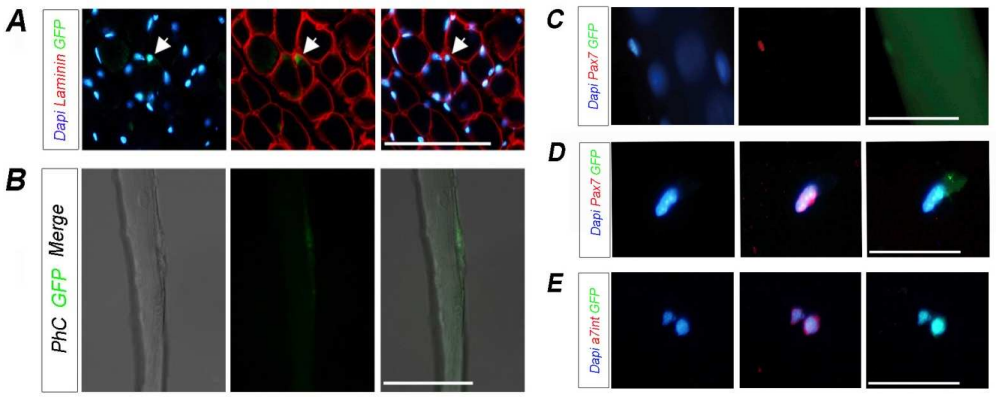

Figure 10: AFS cells differentiate in muscle stem cells. (A) Immunofluorescence of TA muscle from AFS-treated mouse; GFP+ cells are localized in the sub-laminal zone (GFP in green, Laminin

in red). **(B)** Detection of GFP+ cells in isolated fiber. **(C)** Immunofluorescence of Pax7 (red) and GFP (green) in fiber isolated from TA muscle of AFS-treated animal. **(D-E)** Cytospin of SC isolated from TA muscle of AFS-treated mouse. Co-expression of Pax7 and alpha7integrin with GFP demonstrated the differentiation of AFS cells in muscle stem cells. Scale bars =100 µm.

An evaluation of muscle satellite cell population was performed 1 month post-transplantation (4 month-old mice) using Pax7 immunostaining and validated by cytofluorimetric analysis of SM/C-2.6 (*Ikemoto et al., 2007*). As appears in the figure 11, the two data confirmed the PCR analysis reported before (**Figure 8D**) and consistently showed that the number of myogenic progenitors in the AFS-treated muscle is higher (8,05% in AFS-treated vs 0.90% in untreated; **Figure 11**) than in both WT and untreated muscles. The latter is possibly due the exhaustion of satellite cells in the *HSA-Cre, Smn*$^{F7/F7}$ mice which at 4 months show already macroscopical signs of the disease and inevitably die by the age of 9-10 months. This data differ from what has been observed in *mdx* mice (*Reimann et al., 2000*) and Duchenne muscular dystrophy patients (*Kottlors and Kirschner, 2010*), were the number of satellite cells does not decrease even at advanced state of diseases.

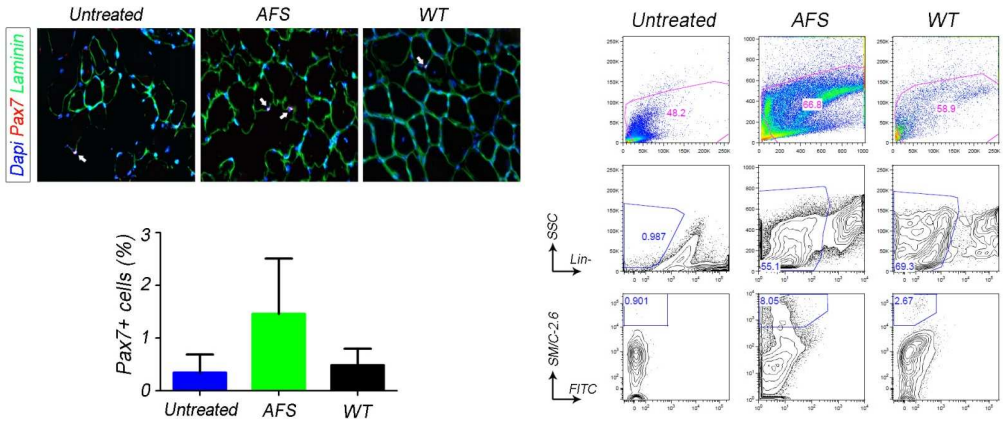

Figure 11: AFS cells trans-differentiate into satellite cells. In AFS-treated muscles were found Pax7+ cells located under the fiber basal lamina and, after digestion of whole muscle, we found GFP+ SM/C-2.6+ cells, indicating that injected cells were able to differentiate in muscle stem cells.

To confirm functional integration of AFS cells in the muscle stem cell niche, both cardiotoxin injury and secondary transplant experiments were performed. In a first set of experiments, cardiotoxin was injected into the TA of BM- and AFS-treated mice 1 month after systemic cell transplantation (**Figure 12A**). Only AFS-treated mice showed newly regenerating GFP+ muscle fibers (51.75% ± 1.35%; **Figure 12B, 12D**) when analyzed 45 days pt, whereas no GFP+ fibers were observed in animals previously transplanted with BM cells (**Figure 12B, 12D**). Moreover, almost all fibers in AFS-transplanted mice were perinucleated 15 days after damage with cardiotoxin. On the contrary, after injury of BM-treated mice, 38.07% ± 2.54% of the regenerating fibers was centrally nucleated (**Figure 12B, 12C**) confirming that only AFS cells were capable of restoring physiological muscle conditions.

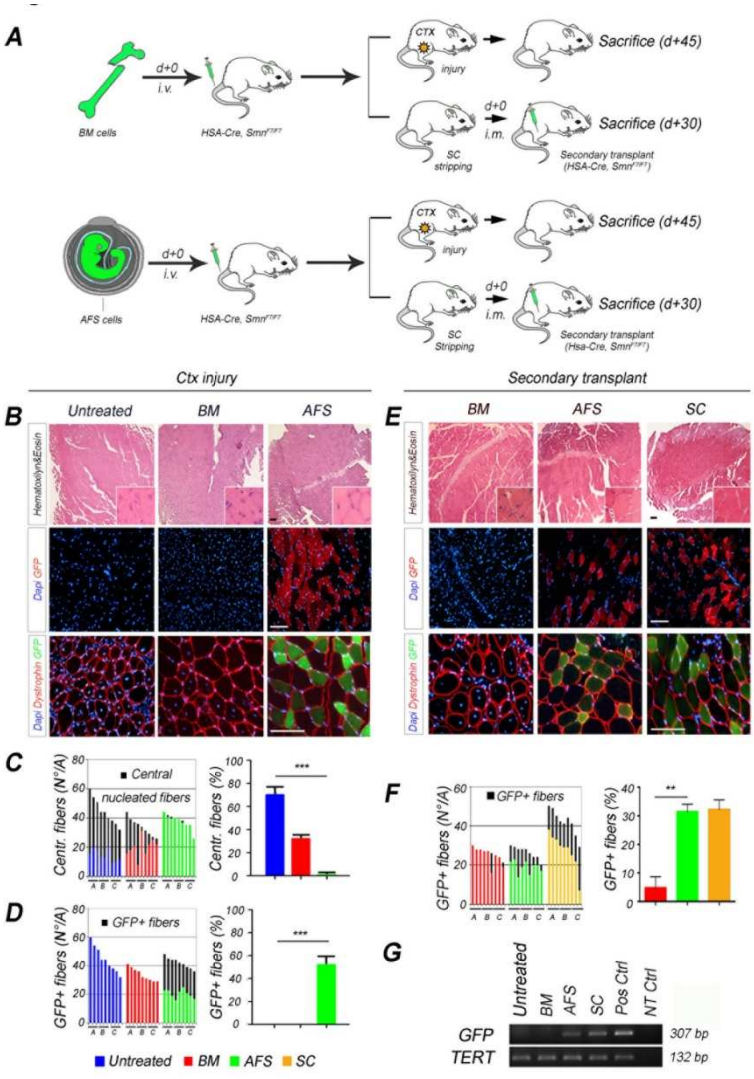

Figure 12: AFS cells fill the muscle stem cell niche. (A) TA muscles of BM- and AFS-treated mice were injured with cardiotoxin (Ctx) 30 days pt and animals were sacrificed 45 days pt. For secondary transplant experiments, primary transplanted mice were sacrificed 30 days pt, satellite cells were isolated from EDL and *Soleus* muscles and injected into secondary *HSA-Cre, Smn*$^{F7/F7}$ hosts, which were sacrificed and analyzed 30 days later. **(B-D)** Ctx injury: Fifteen days after Ctx injury, only AFS-treated mice displayed GFP+ fibers. Graphs of raw number and percentages of central nucleated (untreated 63.70%±3.24; BM-treated 38.07%±6.73; AFS-treated <0.1%; ***p<0.001) and GFP+ fibers (untreated 0%; BM-treated 0%; AFS-treated 51.75%±1.35; ***p<0.001) in untreated, BM- and AFS-treated mice demonstrated that only AFS cells efficiently regenerate skeletal muscle fibers. **(E-F)** Secondary transplants: Thirty days pt, GFP+ fibers were observed in all 6 mice injected with SC derived from AFS-treated mice (31.47%±2.63), but only in one out of 6 mice transplanted with SC derived from BM-treated mice (4.80%±3.86; **p<0.01). Scale bar = 100 µm. A,B,C letters on the x axis in graphs c and e represent an individual muscle evaluated in 3 representative high power fields. **(G)** PCR analysis confirmed that TA muscle treated with SC isolated from primary AFS-treated mice expressed GFP. Amplification of the GFP gene (307 bp) and TERT (132 bp) in TA muscles of untreated, secondary BM-treated (BM), secondary AFS-treated (AFS) and GFP+ SC-treated (SC) *HSA-Cre, Smn*$^{F7/F7}$ mice. (Positive control: genomic DNA from GFP+ AFS cells. NTC=no template control).

To further establish whether AFS cells were truly engrafted into the muscle niche and replaced resident muscle stem cells, secondary transplants were performed (**Figure 12A**). Single myofibers were isolated from BM- (n=6) and AFS- (n=6) transplanted animals and from WT C57BL/6 GFP+ mice (n=3), as previously described (*Montarras et al., 2005; Rossi et al., 2011*). Five hundred freshly isolated SCs, disengaged from single myofibers, were injected locally into TA muscles of naive, 3-month-old *HSA-Cre, Smn*$^{F7/F7}$ mice. One month after secondary transplantation, all the mice in the AFS cell group (n=6) had GFP+ fibers (mean: 31.47% ± 2.63%; **Figure 12E, 12F**) and did not differ significantly from hosts having received WT GFP+ SCs (mean 32.21% ± 3.39%; **Figure 12E, 12F**). In contrast, only one out of six of the recipients of muscle cells derived from BM-treated mice had a few GFP+ fibers (4.80% ± 3.86%). Furthermore, this pattern was confirmed by PCR analysis of GFP genomic DNA in TA muscles of the secondary transplanted animals (**Figure 12G**).

To exclude that AFS cells potential to regenerate skeletal muscle even after cardiotoxin injury was simply related to their fetal origin, c-Kit+ fetal liver (FL)

cells were used as further control. Interestingly, c-Kit+ FL cells did not differ from BM cells and GFP+ fibers were not found after cardiotoxin injury confirming the unique muscle regeneration potential of AFS cells (**Figure 13**).

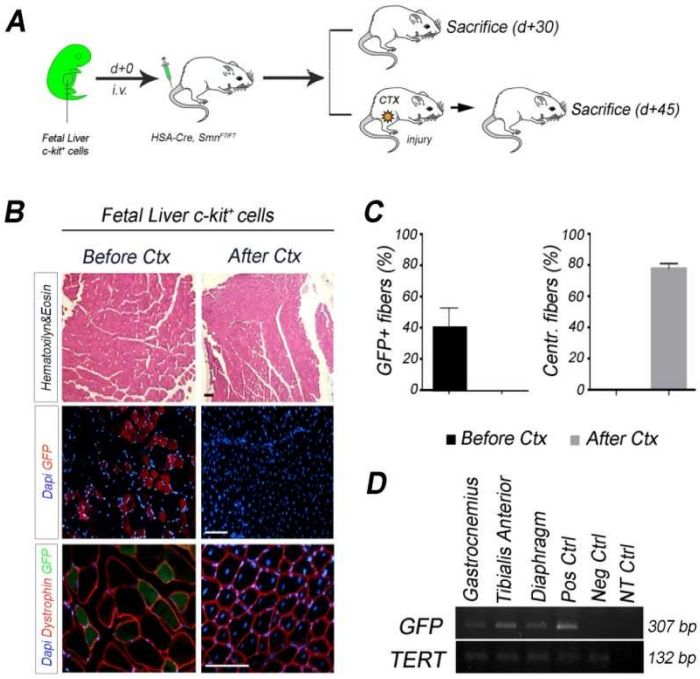

Figure 13: Fetal liver and muscle. (A) FL-treated mice were sacrificed 30 days after transplantation or 15 days after cardiotoxin injury (45 pt). **(B)** One month after systemic injection of c-Kit+ GFP+ Fetal liver cells (FL), TA of mutant mice displayed a relative high number of GFP+ fibers, but 15 days after ctx injury (45 days pt), no GFP+ signal was founded. Scale bar =100 µm. **(C)** Percentage of GFP+ fibers and central nucleated myofibers of TA before and after ctx injury. **(D)** PCR analysis of muscles from FL-treated mice 1 month after cell injection.

5. *In vitro* expanded AFS cells preserve myogenic potential

Given the poor recovery of freshly isolated AFS cells and the strong therapeutic interest, we explored the myogenic potential of *ex vivo*-expanded AFS cells (**Figure 14A**). After 2 weeks of culture on fibroblast feeder layer (**Figure 14B**), AFS cells were sorted for the dual expression of GFP and c-Kit (89.50% ± 6.27%) and then transplanted in 3-month-old *HSA-Cre, Smn*$^{F7/F7}$ mice. Similarly to what had been observed with freshly isolated AFS cells, the muscles of treated mice displayed, 1 month after treatment, a normal phenotype with well-organized

dystrophin expression, less than 1% centrally nucleated fibers, and 21.01% ± 3.57% GFP+ fibers (**Figure 14C, 14D**). Multiple skeletal muscle engraftments in the transplanted animals were also confirmed by PCR analyses of genomic GFP (**Figure 14E**).

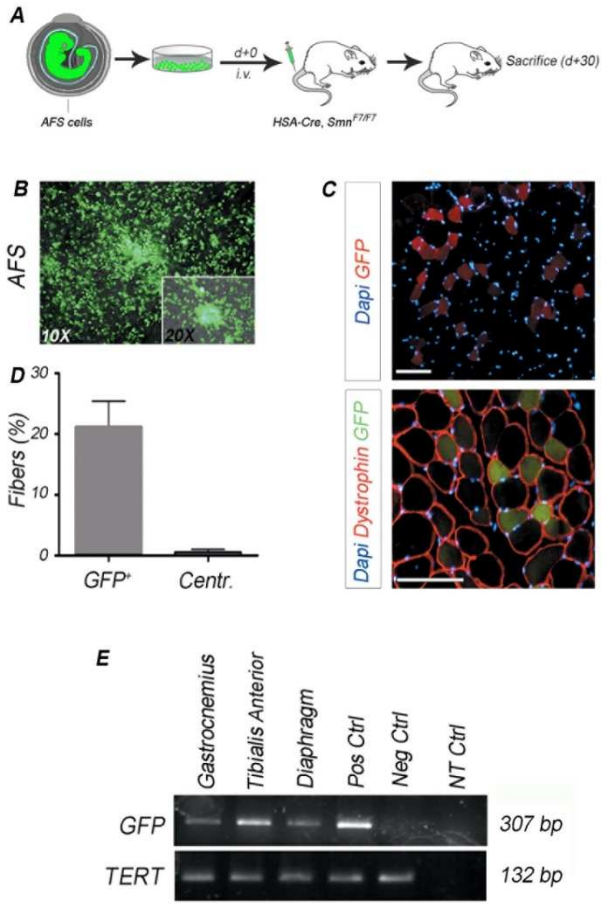

Figure 14: Transplantation of expanded AFS cells generates skeletal muscle tissue. (A) After 15 days of culture, AFS cells GFP+/c-Kit+ were sorted and injected in *HSA-Cre, Smn$^{F7/F7}$* mice. **(B)** GFP+ AFS cells were passaged twice on a mouse embryonic fibroblast feeder layer. Magnification 10X and 20X for the inlet. **(C)** Immunofluorescence with anti-GFP and anti-dystrophin antibodies: 1 month after transplantation, the muscles of treated *HSA-Cre, Smn$^{F7/F7}$* mice displayed a considerable number of GFP+ fibers and a normal levels of dystrophin expression. Scale bar = 100 µm. **(D)** Percentage of GFP+ and central nucleated myofibers in cultured AFS-treated animals. **(E)** PCR analyses of *gastrocnemius*, TA and diaphragm muscles isolated from mice transplanted with cultured AFS cells. First lane: amplification of the GFP gene (307 bp). Second lane: amplification of genomic TERT (132 bp) to confirm the quality of the extracted DNA. For each PCR, the positive control (Pos Ctrl) for GFP amplification was the genomic DNA extracted from GFP+ AFS cells; NTC=no template control.

vii. Discussion

AFS cells represent a small percentage of total amniotic fluid cells (around 1%) that can be harvested by amniocentesis and enriched by immunoselection using anti-CD117 (c-Kit) antibody. Human AFS cells have a high renewal capacity and can be expanded for over 250 doublings without any detectable loss of chromosomal telomere length. We described their potential to give rise, *in vitro*, to a wide range of cell types representing the three primary embryonic lineages of mesoderm, ectoderm and endoderm, and, *in vivo*, to differentiate towards neurogenic and osteogenic lineages (*De Coppi et al., 2007a*). Since the development, especially regarding embryonic annexes, is different among mammals, in this work we deeply explored the stemness characteristics of mouse AFS cells and their therapeutic potential in a model of muscle disease.

Our results strongly suggest that AFS cells, but not BM cells, integrate in the muscle stem cell compartment and have long-term potential for muscle regeneration in *HSA-Cre, Smn*$^{F7/F7}$ mutant mice. This mouse model, which has been extensively characterized, closely replicates the clinical features of human muscular dystrophies. When injected systemically into *HSA-Cre,Smn*$^{F7/F7}$ mutant mice, BM cells were not able to rescue the phenotype and have shown a limited therapeutic efficiency failing to make a substantial, long-term therapeutic contribution (*Salah-Mohellibi et al., 2006*). Unselected and selected BM cell populations have been widely tested in various mouse models of muscle diseases, with an initial enthusiasm prompted by cells' ability to fuse with the host muscle tissue (*Ferrari et al., 1998; Gussoni et al., 1999*) and subsequently activate resident SCs (*Salah-Mohellibi et al., 2006*). However, it is still not clear whether BM cells are able to integrate in the muscle stem cell niche and are capable of regenerating new fibers after damage (*Sherwood et al., 2004; Xynos et al., 2010*). Mesenchymal stem cells from BM and other sources are able to restore dystrophin expression in the *mdx* mouse, but the impact on muscle

repair is dependent on forced expression of MyoD *(Choi et al., 1990; De Bari et al., 2003; Goudenege et al., 2009*). BM stem cells may indeed be therapeutic by producing molecules that regulate muscle regeneration or reduce inflammation, while they are able to establish immune tolerance in a dystrophic animal model and allow stable engraftment of donor muscle-derived cells *(Parker et al., 2008*). More encouraging results have been obtained using stem cells isolated directly from muscle tissue. The intra-arterial delivery of niche-derived mesangioblasts results in morphological and functional correction of the dystrophic phenotype in adult immunocompetent αsarcoglycan null mice (*Sampaolesi et al., 2003*), in SCID/BlAJ mice, a novel model of dysferlinopathy (*Diaz-Manera et al., 2011*), and golden retriever muscular dystrophy dogs (*Sampaolesi et al., 2006*). Alternatively, functional myogenic cells can be also derived from ES cells (*Sakurai et al., 2008*). Intramuscular and systemic transplantation of Pax3+ PDGF-αR+ and Flk1+ ES-derived cells into dystrophic mice results in extensive engraftment of adult myofibers, with enhanced contractile function and no teratoma formation (*Darabi et al., 2008*). In order to overcome the immunological problem related to ES cell transplantation, patient-specific induced pluripotent stem (iPS) cells could also be generated (*Takahashi and Yamanaka, 2006*). Similarly to ES cells, iPS cells can both generate *in vitro* skeletal muscle stem cells, and, after enrichment using the anti-SC antibody SM/C-2.6, functionally engraft into skeletal muscle when transplanted into *mdx* mice (*Darabi et al., 2011; Mizuno et al., 2010*). While ES- and iPS-derived myogenic cells may become useful for therapy in the future, a readily available source of cells with myogenic potential would be relevant as therapeutic alternative to muscle-derived stem cells. Our group has previously demonstrated that (a) broadly multipotent stem cells can be derived from amniotic fluid (*De Coppi et al., 2007a*) and (b) freshly isolated murine AFS cells show hematopoietic potential when injected in Rag1-/- mice (*Ditadi et al., 2009*). AFS cells have been tested in various disease models and have been shown to contribute to organ regeneration (*Carraro et al., 2008; Hauser et al., 2010; Rota et al., 2011*). Similarly to BM cells and mesangioblasts (*Sampaolesi et al., 2006*), AFS cells can cross the endothelial barrier and are therefore suitable for systemic

injection (*Carraro et al., 2008; Ghionzoli et al., 2009*). However, their myogenic potential remains to be fully elucidated. While AFS cells have shown to be able to fuse into myotubes (*De Coppi et al., 2007a*), Gekas *et al.* failed to show functional engraftment of human AFS cells after expansion when injected in immunocompromised animals (*Gekas et al., 2010*). Differently, we show that murine AFS cells are able to restore muscle function in a model of disease and to maintain a long-lasting therapeutic efficiency possibly because of their unique ability of switching toward muscle stem cells. The beneficial effects are tightly correlated with the normalization of pathological skeletal muscle regeneration and the remarkable attenuation of mutant phenotype (treated animals showed neither kyphosis nor abdominal shrink) resulting in the long-term survival observed here. We first hypothesized that muscle progenitors were present among the AFS cells, but, immediately after c-Kit selection, the AFS cells' gene expression profile was not suggestive of any myogenic commitment within the population.

It is noteworthy that after intravenous cell injection (and despite differences in the number of injected cells), BM- and AFS-treated animals possessed similar numbers of perinucleated fibers, highlighting the positive effect of cell treatment. However, the functional engraftment of the two cell types in the affected muscles differs drastically and in order to explain the long-lasting effect of AFS cell transplantation, we hypothesized that the fetal cells (in contrast to BM cells) were able to migrate into the muscle stem cell niche. This behavior is a feature not only of SCs (*Collins et al., 2005*) but also of other stem cells of muscle origins (*Cerletti et al., 2008*) or perycites, as previously demonstrated (*Dellavalle et al., 2011*). Therefore, the finding of GFP+ cells in sub-laminal position warrant our theory. Despite the presence of stem cell progenitors in the BM, our selected population of fetal stem cells appears to be more efficient. In fact, 50% of the BM-treated mice survived for 18 months, in contrast with 75% of the AFS-treated mice. Moreover, only AFS-injected muscles still had a high proportion (approximately 60%) of GFP+ fibers more than a year after transplantation. The high number of central nucleated fibers observed in BM-treated animals after

cardiotoxin injection proved that BM cells failed to functionally integrate into the muscle stem cell niche (*Sherwood et al., 2004; Xynos et al., 2010*), whereas GFP+ fibers in AFS-treated muscle resulted not only from cell fusion, but also from *de novo* fiber generation from newly born muscle stem cells. Moreover, the higher AFS cell muscle engraftment indicated that a strong ablative preconditioning injury enhances the therapeutic effect—possibly because of the selective advantage of functionally normal cells in AFS-treated mice. Integration of AFS cells in the stem cell niche is also confirmed by secondary transplants in *HSA-Cre, $Smn^{F7/F7}$* mice of SCs isolated from BM- and AFS-treated animals. Only the latter group consistently showed the ability of AFS-derived SCs to form new fibers, similarly to what observed in mice injected with SCs derived from C57BL/6 GFP+ mice. While SCs have been isolated according to a well-established protocol (*Collins et al., 2005*), we are limited by not using a SCs lineage tracing mouse for isolating AFS-derived SCs (*Darabi et al., 2008*).

In order to progress toward AFS cells application for therapy, it was also important to establish if their myogenic potential could be preserved after expansion, as it has been recently demonstrated for alkaline phosphatase positive pericytes (*Dellavalle et al., 2011; Sampaolesi et al., 2006*). Accordingly, *in vitro* expanded AFS cells demonstrated the maintenance of regenerative properties after intravenous injection in *HSA-Cre, $Smn^{F7/F7}$* mutant mice . Twenty percent of the fibers was of donor origin, a remarkable result, given that (a) some adult stem and progenitor cells have proved difficult to expand in culture and (b) skeletal muscle SCs multiply rapidly in culture but show diminished regenerative capacity when transplanted *in vivo* (*Montarras et al., 2005*). Nevertheless, 20% was lower than the value achieved in animals having received freshly isolated AFS cells. Further work is required to assess the relationship between myogenic potential and expansion conditions. Moreover, while it is clear that AFS cells are capable of restoring normal muscle function in *HSA-Cre, $Smn^{F7/F7}$* mutant mice primarily by engraftment and differentiation, future work will need to address whether bystender effect also has a role in this animal

model of disease since it is possible that AFS cells could also activate resident Pax7+ SCs (similarly to what has been described for BM cells) (*Yoon et al., 2009*).

In conclusion, AFS cells may constitute a promising therapeutic option for muscle regeneration, since (a) systemic injection of low cell numbers clearly replenishes the muscle stem cell niche and (b) cultured AFS cells also seem to possess a high regeneration capacity. These results are relevant for the development of efficient treatment of muscle disease where an alternative to SCs is needed because of their limitation to be expanded and to migrate through the endothelial barrier. In depth studies must be now performed with human AFS cells to verify if this new source of stem cells can open unexpected and highly required therapeutic approaches for devastating disease like those affecting the skeletal muscle tissue.

vii. Bibliography

Blaauw, B., Mammucari, C., Toniolo, L., Agatea, L., Abraham, R., Sandri, M., Reggiani, C. and Schiaffino, S. (2008). Akt activation prevents the force drop induced by eccentric contractions in dystrophin-deficient skeletal muscle. *Hum Mol Genet* **17**, 3686-96.

Bollini, S., Pozzobon, M., Nobles, M., Riegler, J., Dong, X., Piccoli, M., Chiavegato, A., Price, A. N., Ghionzoli, M., Cheung, K. K. et al. (2010). In vitro and in vivo cardiomyogenic differentiation of amniotic fluid stem cells. *Stem Cell Rev* **7**, 364-80.

Carraro, G., Perin, L., Sedrakyan, S., Giuliani, S., Tiozzo, C., Lee, J., Turcatel, G., De Langhe, S. P., Driscoll, B., Bellusci, S. et al. (2008). Human amniotic fluid stem cells can integrate and differentiate into epithelial lung lineages. *Stem Cells* **26**, 2902-11.

Cerletti, M., Jurga, S., Witczak, C. A., Hirshman, M. F., Shadrach, J. L., Goodyear, L. J. and Wagers, A. J. (2008). Highly efficient, functional engraftment of skeletal muscle stem cells in dystrophic muscles. *Cell* **134**, 37-47.

Chiavegato, A., Bollini, S., Pozzobon, M., Callegari, A., Gasparotto, L., Taiani, J., Piccoli, M., Lenzini, E., Gerosa, G., Vendramin, I. et al. (2007). Human amniotic fluid-derived stem cells are rejected after transplantation in the myocardium of normal, ischemic, immuno-suppressed or immuno-deficient rat. *J Mol Cell Cardiol* **42**, 746-59.

Choi, J., Costa, M. L., Mermelstein, C. S., Chagas, C., Holtzer, S. and Holtzer, H. (1990). MyoD converts primary dermal fibroblasts, chondroblasts, smooth muscle, and retinal pigmented epithelial cells into striated mononucleated myoblasts and multinucleated myotubes. *Proc Natl Acad Sci U S A* **87**, 7988-92.

Collins, C. A., Olsen, I., Zammit, P. S., Heslop, L., Petrie, A., Partridge, T. A. and Morgan, J. E. (2005). Stem cell function, self-renewal, and behavioral heterogeneity of cells from the adult muscle satellite cell niche. *Cell* **122**, 289-301.

Crawford, T. O. (2004). Concerns about the design of clinical trials for spinal muscular atrophy. *Neuromuscul Disord* **14**, 456-60.

Darabi, R., Gehlbach, K., Bachoo, R. M., Kamath, S., Osawa, M., Kamm, K. E., Kyba, M. and Perlingeiro, R. C. (2008). Functional skeletal muscle regeneration from differentiating embryonic stem cells. *Nat Med* **14**, 134-43.

Darabi, R., Pan, W., Bosnakovski, D., Baik, J., Kyba, M. and Perlingeiro, R. C. (2011). Functional myogenic engraftment from mouse iPS cells. *Stem Cell Rev* **7**, 948-57.

De Bari, C., Dell'Accio, F., Vandenabeele, F., Vermeesch, J. R., Raymackers, J. M. and Luyten, F. P. (2003). Skeletal muscle repair by adult human mesenchymal stem cells from synovial membrane. *J Cell Biol* **160**, 909-18.

De Coppi, P., Bartsch, G., Jr., Siddiqui, M. M., Xu, T., Santos, C. C., Perin, L., Mostoslavsky, G., Serre, A. C., Snyder, E. Y., Yoo, J. J. et al. (2007a). Isolation of amniotic stem cell lines with potential for therapy. *Nat Biotechnol* **25**, 100-6.

De Coppi, P., Callegari, A., Chiavegato, A., Gasparotto, L., Piccoli, M., Taiani, J., Pozzobon, M., Boldrin, L., Okabe, M., Cozzi, E. et al. (2007b). Amniotic fluid and bone marrow derived mesenchymal stem cells can be converted to smooth muscle cells in the cryo-injured rat bladder and prevent compensatory hypertrophy of surviving smooth muscle cells. *J Urol* **177**, 369-76.

De Rosa, L. and De Luca, M. (2012). Cell biology: Dormant and restless skin stem cells. *Nature* **489**, 215-7.

Dellavalle, A., Maroli, G., Covarello, D., Azzoni, E., Innocenzi, A., Perani, L., Antonini, S., Sambasivan, R., Brunelli, S., Tajbakhsh, S. et al. (2011). Pericytes resident in postnatal skeletal muscle differentiate into muscle fibres and generate satellite cells. *Nat Commun* **2**, 499.

Diaz-Manera, J., Touvier, T., Dellavalle, A., Tonlorenzi, R., Tedesco, F. S., Messina, G., Meregalli, M., Navarro, C., Perani, L., Bonfanti, C. et al. (2011). Partial dysferlin reconstitution by adult murine mesoangioblasts is sufficient for full functional recovery in a murine model of dysferlinopathy. *Cell Death Dis* **1**, e61.

DiDonato, C. J., Chen, X. N., Noya, D., Korenberg, J. R., Nadeau, J. H. and Simard, L. R. (1997). Cloning, characterization, and copy number of the murine survival motor neuron gene: homolog of the spinal muscular atrophy-determining gene. *Genome Res* **7**, 339-52.

Ditadi, A., de Coppi, P., Picone, O., Gautreau, L., Smati, R., Six, E., Bonhomme, D., Ezine, S., Frydman, R., Cavazzana-Calvo, M. et al. (2009). Human and murine amniotic fluid c-Kit+Lin- cells display hematopoietic activity. *Blood* **113**, 3953-60.

Ferrari, G., Cusella-De Angelis, G., Coletta, M., Paolucci, E., Stornaiuolo, A., Cossu, G. and Mavilio, F. (1998). Muscle regeneration by bone marrow-derived myogenic progenitors. *Science* **279**, 1528-30.

Friedenstein, A. J., Ivanov-Smolenski, A. A., Chajlakjan, R. K., Gorskaya, U. F., Kuralesova, A. I., Latzinik, N. W. and Gerasimow, U. W. (1978). Origin of bone marrow stromal mechanocytes in radiochimeras and heterotopic transplants. *Exp Hematol* **6**, 440-4.

Gekas, J., Walther, G., Skuk, D., Bujold, E., Harvey, I. and Bertrand, O. F. (2010). In vitro and in vivo study of human amniotic fluid-derived stem cell differentiation into myogenic lineage. *Clin Exp Med* **10**, 1-6.

Ghionzoli, M., Cananzi, M., Zani, A., Rossi, C. A., Leon, F. F., Pierro, A., Eaton, S. and De Coppi, P. (2009). Amniotic fluid stem cell migration after intraperitoneal injection in pup rats: implication for therapy. *Pediatr Surg Int* **26**, 79-84.

Goudenege, S., Pisani, D. F., Wdziekonski, B., Di Santo, J. P., Bagnis, C., Dani, C. and Dechesne, C. A. (2009). Enhancement of myogenic and muscle repair capacities of human adipose-derived stem cells with forced expression of MyoD. *Mol Ther* **17**, 1064-72.

Grinnemo, K. H., Sylven, C., Hovatta, O., Dellgren, G. and Corbascio, M. (2008). Immunogenicity of human embryonic stem cells. *Cell Tissue Res* **331**, 67-78.

Gussoni, E., Soneoka, Y., Strickland, C. D., Buzney, E. A., Khan, M. K., Flint, A. F., Kunkel, L. M. and Mulligan, R. C. (1999). Dystrophin expression in the mdx mouse restored by stem cell transplantation. *Nature* **401**, 390-4.

Hauser, P. V., De Fazio, R., Bruno, S., Sdei, S., Grange, C., Bussolati, B., Benedetto, C. and Camussi, G. (2010). Stem cells derived from human amniotic fluid contribute to acute kidney injury recovery. *Am J Pathol* **177**, 2011-21.

Ikemoto, M., Fukada, S., Uezumi, A., Masuda, S., Miyoshi, H., Yamamoto, H., Wada, M. R., Masubuchi, N., Miyagoe-Suzuki, Y. and Takeda, S. (2007). Autologous transplantation of SM/C-2.6(+) satellite cells transduced with micro-dystrophin CS1 cDNA by lentiviral vector into mdx mice. *Mol Ther* **15**, 2178-85.

In 't Anker, P. S., Scherjon, S. A., Kleijburg-van der Keur, C., Noort, W. A., Claas, F. H., Willemze, R., Fibbe, W. E. and Kanhai, H. H. (2003). Amniotic fluid as a novel source of mesenchymal stem cells for therapeutic transplantation. *Blood* **102**, 1548-9.

Kottlors, M. and Kirschner, J. (2010). Elevated satellite cell number in Duchenne muscular dystrophy. *Cell Tissue Res* **340**, 541-8.

Mauro, A. (1961). Satellite cell of skeletal muscle fibers. *J Biophys Biochem Cytol* **9**, 493-5.

Mizuno, Y., Chang, H., Umeda, K., Niwa, A., Iwasa, T., Awaya, T., Fukada, S., Yamamoto, H., Yamanaka, S., Nakahata, T. et al. (2010). Generation of skeletal muscle stem/progenitor cells from murine induced pluripotent stem cells. *FASEB J* **24**, 2245-53.

Montarras, D., Morgan, J., Collins, C., Relaix, F., Zaffran, S., Cumano, A., Partridge, T. and Buckingham, M. (2005). Direct isolation of satellite cells for skeletal muscle regeneration. *Science* **309**, 2064-7.

Nicole, S., Desforges, B., Millet, G., Lesbordes, J., Cifuentes-Diaz, C., Vertes, D., Cao, M. L., De Backer, F., Languille, L., Roblot, N. et al. (2003). Intact satellite cells lead to remarkable protection against Smn gene defect in differentiated skeletal muscle. *J Cell Biol* **161**, 571-82.

Parker, M. H., Kuhr, C., Tapscott, S. J. and Storb, R. (2008). Hematopoietic cell transplantation provides an immune-tolerant platform for myoblast transplantation in dystrophic dogs. *Mol Ther* **16**, 1340-6.

Reimann, J., Irintchev, A. and Wernig, A. (2000). Regenerative capacity and the number of satellite cells in soleus muscles of normal and mdx mice. *Neuromuscul Disord* **10**, 276-82.

Rossi, C. A., Flaibani, M., Blaauw, B., Pozzobon, M., Figallo, E., Reggiani, C., Vitiello, L., Elvassore, N. and De Coppi, P. (2011). In vivo tissue engineering of functional skeletal muscle by freshly isolated satellite cells embedded in a photopolymerizable hydrogel. *FASEB J* **25**, 2296-304.

Rota, C., Imberti, B., Pozzobon, M., Piccoli, M., De Coppi, P., Atala, A., Gagliardini, E., Xinaris, C., Benedetti, V., Fabricio, A. S. et al. (2011). Human amniotic fluid stem cell preconditioning improves their regenerative potential. *Stem Cells Dev* **21**, 1911-23.

Sacco, A., Mourkioti, F., Tran, R., Choi, J., Llewellyn, M., Kraft, P., Shkreli, M., Delp, S., Pomerantz, J. H., Artandi, S. E. et al. (2010). Short telomeres and stem cell exhaustion model Duchenne muscular dystrophy in mdx/mTR mice. *Cell* **143**, 1059-71.

Sakurai, H., Okawa, Y., Inami, Y., Nishio, N. and Isobe, K. (2008). Paraxial mesodermal progenitors derived from mouse embryonic stem cells contribute to muscle regeneration via differentiation into muscle satellite cells. *Stem Cells* **26**, 1865-73.

Salah-Mohellibi, N., Millet, G., Andre-Schmutz, I., Desforges, B., Olaso, R., Roblot, N., Courageot, S., Bensimon, G., Cavazzana-Calvo, M. and Melki, J. (2006). Bone marrow transplantation attenuates the myopathic phenotype of a muscular mouse model of spinal muscular atrophy. *Stem Cells* **24**, 2723-32.

Sampaolesi, M., Blot, S., D'Antona, G., Granger, N., Tonlorenzi, R., Innocenzi, A., Mognol, P., Thibaud, J. L., Galvez, B. G., Barthelemy, I. et al. (2006). Mesoangioblast stem cells ameliorate muscle function in dystrophic dogs. *Nature* **444**, 574-9.

Sampaolesi, M., Torrente, Y., Innocenzi, A., Tonlorenzi, R., D'Antona, G., Pellegrino, M. A., Barresi, R., Bresolin, N., De Angelis, M. G., Campbell, K. P. et al. (2003). Cell therapy of alpha-sarcoglycan null dystrophic mice through intra-arterial delivery of mesoangioblasts. *Science* **301**, 487-92.

Schrank, B., Gotz, R., Gunnersen, J. M., Ure, J. M., Toyka, K. V., Smith, A. G. and Sendtner, M. (1997). Inactivation of the survival motor neuron gene, a candidate gene for human spinal muscular atrophy, leads to massive cell death in early mouse embryos. *Proc Natl Acad Sci U S A* **94**, 9920-5.

Sherwood, R. I., Christensen, J. L., Conboy, I. M., Conboy, M. J., Rando, T. A., Weissman, I. L. and Wagers, A. J. (2004). Isolation of adult mouse myogenic progenitors: functional heterogeneity of cells within and engrafting skeletal muscle. *Cell* **119**, 543-54.

Siegel, G., Krause, P., Wohrle, S., Nowak, P., Ayturan, M., Kluba, T., Brehm, B. R., Neumeister, B., Kohler, D., Rosenberger, P. et al. (2012). Bone marrow-derived human mesenchymal stem cells express cardiomyogenic proteins but do not exhibit functional cardiomyogenic differentiation potential. *Stem Cells Dev* **21**, 2457-70.

Takahashi, K. and Yamanaka, S. (2006). Induction of pluripotent stem cells from mouse embryonic and adult fibroblast cultures by defined factors. *Cell* **126**, 663-76.

Viollet, L., Bertrandy, S., Bueno Brunialti, A. L., Lefebvre, S., Burlet, P., Clermont, O., Cruaud, C., Guenet, J. L., Munnich, A. and Melki, J. (1997). cDNA isolation, expression, and chromosomal localization of the mouse survival motor neuron gene (Smn). *Genomics* **40**, 185-8.

Xynos, A., Corbella, P., Belmonte, N., Zini, R., Manfredini, R. and Ferrari, G. (2010). Bone marrow-derived hematopoietic cells undergo myogenic differentiation following a Pax-7 independent pathway. *Stem Cells* **28**, 965-73.

Yamanaka, S. (2010). Patient-specific pluripotent stem cells become even more accessible. *Cell Stem Cell* **7**, 1-2.

Yoon, B. S., Moon, J. H., Jun, E. K., Kim, J., Maeng, I., Kim, J. S., Lee, J. H., Baik, C. S., Kim, A., Cho, K. S. et al. (2009). Secretory profiles and wound healing effects of human amniotic fluid-derived mesenchymal stem cells. *Stem Cells Dev* **19**, 887-902.

Zani, A., Cananzi, M., Fascetti-Leon, F., Lauriti, G., Smith, V. V., Bollini, S., Ghionzoli, M., D'Arrigo, A., Pozzobon, M., Piccoli, M. et al. (2013). Amniotic fluid stem cells improve survival and enhance repair of damaged intestine in necrotising enterocolitis via a COX-2 dependent mechanism. *Gut*.

Zuk, P. A., Zhu, M., Ashjian, P., De Ugarte, D. A., Huang, J. I., Mizuno, H., Alfonso, Z. C., Fraser, J. K., Benhaim, P. and Hedrick, M. H. (2002). Human adipose tissue is a source of multipotent stem cells. *Mol Biol Cell* **13**, 4279-95.